Journal of Physics D: Applied Physics

Hole density and acceptor-type defects in MBE-grown $GaSb_{1-x}Bi_x$

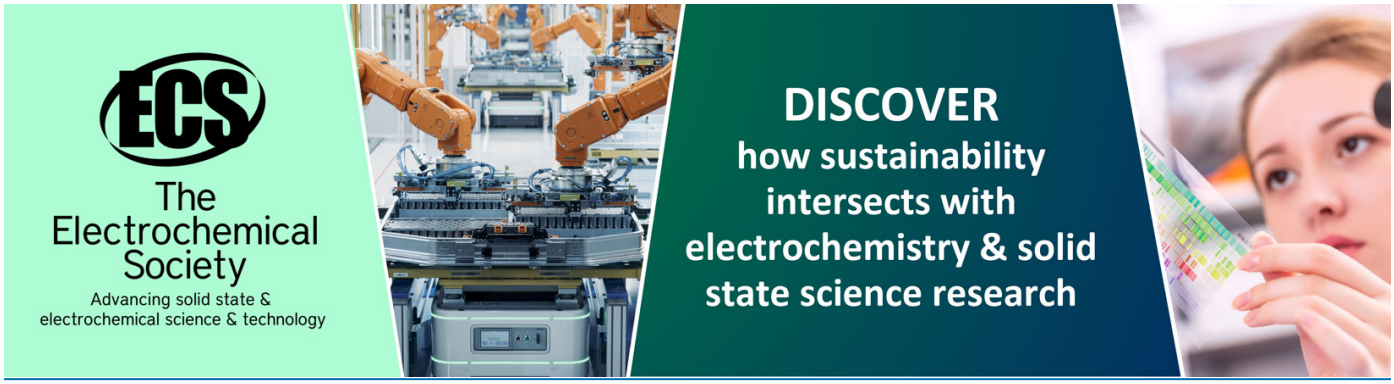

OPEN ACCESS
IOP Publishing
Journal of Physics D: Applied Physics
J. Phys. D: Appl. Phys. **50** (2017) 295102 (6pp)
https://doi.org/10.1088/1361-6463/aa779a

Hole density and acceptor-type defects in MBE-grown $GaSb_{1-x}Bi_x$

N Segercrantz[1], J Slotte[1], I Makkonen[1], F Tuomisto[1], I C Sandall[2], M J Ashwin[3] and T D Veal[4]

[1] Department of Applied Physics, Aalto University School of Science, PO Box 15100, FIN-00076 Aalto Finland
[2] Department of Electrical Engineering and Electronics, University of Liverpool, Liverpool, L69 3GJ, United Kingdom
[3] Department of Physics, University of Warwick, Coventry, CV4 7AL, United Kingdom
[4] Department of Physics and Stephenson Institute for Renewable Energy, University of Liverpool, Liverpool, L69 7ZF, United Kingdom

E-mail: natalie.segercrantz@aalto.fi

Received 22 February 2017, revised 18 May 2017
Accepted for publication 6 June 2017
Published 3 July 2017

Abstract

We study acceptor-type defects in $GaSb_{1-x}Bi_x$ grown by molecular beam epitaxy. The hole density of the $GaSb_{1-x}Bi_x$ layers, from capacitance-voltage measurements of Schottky diodes, is higher than that of the binary alloys and increases linearly up to 10^{19} cm^{-3} with the Bi content. Positron annihilation spectroscopy and *ab initio* calculations show that both Ga vacancies and Ga antisites contribute to the hole density and that the proportion of the two acceptor-type defects vary in the layers. The modification of the band gap due to Bi incorporation as well as the growth parameters are suggested to affect the concentrations of acceptor-type defects.

Keywords: GaSb, GaSbBi, defects, positron annihilation spectroscopy

(Some figures may appear in colour only in the online journal)

Introduction

Adding Bi to III–V semiconductors has shown to provide a means for effectively tuning the band gap thereby making such alloys attractive for optoelectronic devices [1–4]. In addition to the band gap reduction, the Bi-containing alloys are in general of interest due to their large spin–orbit splitting [5, 6]. For $GaSb_{1-x}Bi_x$, a band gap reduction of ~30 meV/% Bi has been reported [7–9] making the material a promising candidate for applications in the 2–5 μm spectral region. The valence band anticrossing in $GaSb_{1-x}Bi_x$ may offer increased hole confinement in devices compared to that available using GaInAsSb [7].

Undoped GaSb is *p*-type irrespective of the growth method and some efforts have been made to find the defect responsible for the residual hole concentration [10–20]. Experimental as well as theoretical work has recently showed that the gallium antisite (Ga_{Sb}) and the gallium vacancy (V_{Ga}) are the prevalent acceptor-type defects [15, 19–21]. By performing *ab initio* calculations, Virkkala *et al* [15] studied the energetics of different native defects in GaSb and estimated the formation energy of the Ga_{Sb} to be considerably low. Acceptor-type defects in Czochralski-grown (CZ)-GaSb were studied by Kujala *et al* [20]. They found the concentration of Ga antisites to be one order of magnitude higher than the V_{Ga} concentration making the antisite the main cause of the *p*-type behavior. In GaSb layers grown by molecular beam epitaxy (MBE) the Ga vacancy was shown to play a more significant part in the *p*-type conductivity [19].

In this article, acceptor-type defects in MBE-grown $GaSb_{1-x}Bi_x$ epitaxial layers are investigated using electrical and positron measurements as well as *ab initio* calculations. Compared to binary GaSb, a significant increase in the hole density is reported for the layers. Both Ga vacancies and Ga

Table 1. Information on the Bi-flux series layers.

Bi content (%)	Bi flux (mbar)	T_G (°C)	Growth rate (μmh^{-1})
1.6	2.0×10^{-8}	275	1.0
2.2	2.6×10^{-8}	275	1.0
2.7	3.5×10^{-8}	275	1.0
3.6	4.1×10^{-8}	275	1.0

Table 2. Information on the growth-temperature series layers.

Bi content (%)	Bi flux (mbar)	T_G (°C)	Growth rate (μmh^{-1})
0.7	3.3×10^{-8}	350	0.4
2.8	3.3×10^{-8}	325	0.4
3.6	3.3×10^{-8}	300	0.4
5.0	3.3×10^{-8}	275	0.4
5.0	3.3×10^{-8}	250	0.4

antisites are found to contribute to the *p*-type conductivity and the proportion of the acceptor-type defects ($[V_{Ga}]/[Ga_{Sb}]$) is found to vary in the $GaSb_{1-x}Bi_x$ layers. Both the growth conditions and the modified band gap of the ternary alloys are suggested to affect the concentrations of the acceptor-type defects.

Experimental details

The studied samples consisted of two series of undoped, MBE-grown $GaSb_{1-x}Bi_x$ epitaxial layers grown on GaSb (0 0 1) undoped substrates. One of the series was grown under a fixed growth temperature ($T_G = 275$ °C) and rate, but with the Bi flux (beam equivalent pressure) varied between samples (hereafter denoted Bi-flux series). The Bi content in the layers was found to increase with the Bi flux. The thickness of these layers is 400 nm. For the second series, the growth temperature was varied 250–350 °C while the other two parameters were kept constant (hereafter denoted growth-temperature series). For these layers, decreasing the growth temperature was shown to increase the Bi content in the layers. At growth temperatures below ~275 °C, the Bi content saturated to $x = 0.05$. The thickness of these layers is 330 nm. Information on growth parameters and the resulting Bi content for both series are shown in the tables 1 and 2, respectively. The surface morphology of the samples, along with further details of the growth and the determination of the Bi content, were investigated in [7, 22]. Rutherford backscattering spectrometry data indicate that the $GaSb_{1-x}Bi_x$ layers are of high crystalline quality with >98% of the incorporated Bi substitutional on the group V sublattice. Scanning electron microscope and atomic force microscope data show that the layers are droplet-free with smooth surfaces. A reference series of four undoped GaSb layers grown at a fixed growth rate of 0.5 μmh^{-1} and at temperatures between 250–400 °C with a thickness of 400 nm was also studied.

To determine the carrier-type and density, the samples were fabricated into Schottky diodes and their capacitance–voltage (C–V) characteristics were measured. Hall effect was not used due to the presence of a conducting GaSb substrate. For the fabrication of Schottky diodes, the GaSb wafers were chemically cleaned before the deposition of the backside Ohmic contact metal via thermal evaporation. The Ohmic contact was realized by evaporating contacts on the back surface of the substrate. Before the deposition of the top Schottky contact, the wafer was cleaned in solvents before being rinsed in HCl solution to remove the native oxide on the substrate. The Schottky contact (Ti/Au), was then thermally evaporated through a metal mask to define circular contacts with a diameter of 100 μm. C–V measurements were performed at room temperature over a range of AC frequencies (100 kHz–2 MHz). The amplitude of the AC Voltage was 50 mV. Measurements were restricted to a maximum reverse voltage of 1 V to protect the devices. From the polarity of the diodes the GaSbBi layers were determined to be *p*-type and from the slope of the $1/C^2$ plot the carrier concentrations were determined using the Mott–Schottky relationship. Only devices exhibiting a phase angle greater than 80° for the entire voltage sweep were used for subsequent calculations.

Positron annihilation spectroscopy was employed for studying defects present in the epitaxial layers. The method is a versatile tool for studying point defects also in narrow band gap semiconductors such as GaSb and its alloys due to the selective sensitivity to open-volume defects and negative ions and the insensitivity to conductivity and band gap width. Positrons can get trapped and annihilate at neutral and negatively charged vacancy defects due to the locally reduced Coulomb repulsion. Negative ions can also localize positrons in hydrogen-like Rydberg states. Measuring the Doppler-broadened 511 keV-annihilation line provides information on the positron trapping defects in the studied material. The thermal positron in the material has negligible momentum, however the momentum of the electron results in a Doppler broadened annihilation line. If trapped by a vacancy, the positron wavefunction has a reduced overlap with core electrons compared to that a delocalized positron in a defect-free lattice leading to a decrease in annihilation with high-momentum core electrons. As the high-momentum part of the Doppler broadening spectrum arises mainly from annihilations with core electrons, information on the chemical identity of the atoms close to the annihilation site of the positron can be obtained. For a more thorough discussion on the technique, see [23].

The Doppler broadening measurements were conducted using a monoenergetic variable energy slow positron beam equipped with a HPGe (high-purity germanium) detector that had an energy resolution of 1.15 keV at 511 keV. For describing results reported in this article, the conventional line-shape parameters *S* and *W* are used. The *S* parameter is defined as the fraction of annihilation events in the central region of the peak thus mainly describing positrons annihilating with low momentum valence electrons. The *W* parameter is defined in a similar manner as the fraction of annihilation events in the high momentum region. The *S* parameter window was set to $|p| < 0.4$ a.u. and the *W* parameter window to 1.6 a.u. $< |p| < 4.0$ a.u. For positrons trapped at vacancies, the overlap with core electron is reduced causing the

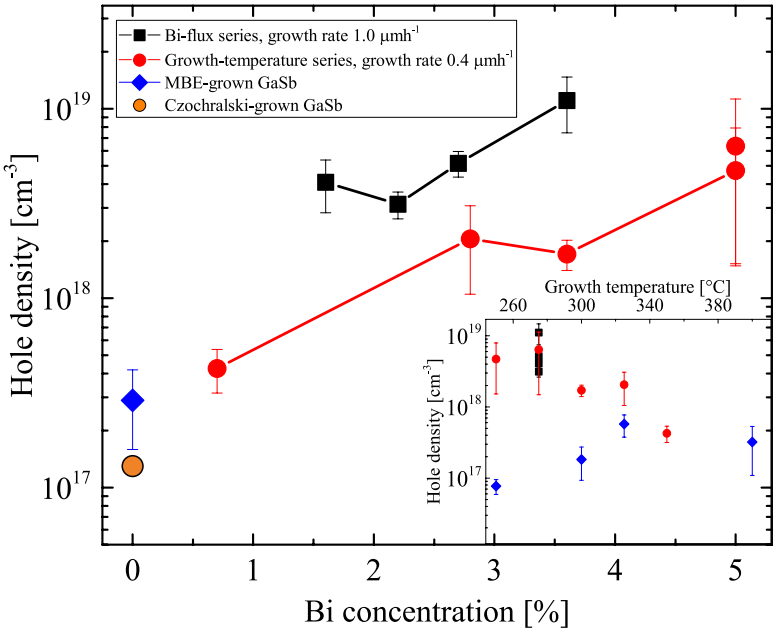

Figure 1. Measured hole density as a function of Bi content for the studied epitaxial layers. An average value for the GaSb layers is also shown as well as the hole density for CZ-GaSb [20]. The inset shows the hole density as a function of growth temperature for the films. The error bars are the standard deviation of measurements of multiple devices fabricated from the same sample.

Doppler broadening spectrum to narrow compared to that of a defect-free bulk. This is usually seen as an increase in the *S* parameter and a decrease in the *W* parameter.

In order to improve the measured peak-to-background ratio and thereby achieve a higher statistical accuracy of the high-momentum region, coincidence Doppler broadening measurements were carried out. For detecting both annihilation photons, a variable energy slow positron beam equipped with a HPGe–detector with resolution 1.2 keV at 511 keV was gated by the signal from another detector. For each spectrum, 10^6 and 10^7 annihilation events were collected for the conventional and coincidence measurements, respectively.

Results

The measured hole density as a function of Bi content for the studied $GaSb_{1-x}Bi_x$ layers is illustrated in figure 1. The average value calculated for the GaSb layers is also shown, alongside the hole density of CZ-GaSb [20]. The hole densities of the $GaSb_{1-x}Bi_x$ layers are clearly higher than those of these binary GaSb samples. For both series, the hole density increases almost monotonically with Bi content. The measured values for the growth-temperature series is lower than for the Bi-flux series. When comparing the two series with each other, the hole density does not seem to solely depend on the the Bi content in the layer. The inset of figure 1 shows the hole density of the layers as a function of growth temperature. $GaSb_{1-x}Bi_x$ layers grown at higher temperatures have somewhat lower hole densities. For the GaSb epitaxial layers, the hole density is in the 10^{17} cm^{-3} range, with a slightly increasing trend with growth temperature.

Results from the Doppler broadening measurements of the Bi-flux and growth-temperature series are shown in figures 2(a) and (b), respectively. The *S* parameter curves for the GaSb layers grown at different temperatures, not shown here, are very similar. Thus, the concentrations of positron trapping defects in the GaSb layers do not seem to be affected by the growth temperature. The figures display the *S* parameter of the binary GaSb layers calculated as an average in the energy range $3\,\text{keV} \leqslant E \leqslant 10\,\text{keV}$ (dashed line) along with the *p*-type GaSb substrate value (dotted line).

For the $GaSb_{1-x}Bi_x$ layers, the *S* parameters seem to depend on the Bi content in the epitaxial layers. A similar dependence, not shown here, was observed for the *W* parameter. At energies $3\,\text{keV} \leqslant E \leqslant 10$ keV, the measured signal mostly consists of positrons annihilating in the epitaxial layer. The value of the *S* parameter measured at these energies is similar for samples with similar Bi content and almost independent of the growth parameters. The *S* parameter value of the two samples with 5% Bi grown at different temperatures is, for example, very similar. For samples with Bi contents in the range of 0.7–3.6%, the *S* parameter increases as the Bi content in the layers increases. However, the *S* parameter values of the samples with highest Bi contents of 5% are similar to these of the lowest Bi content layers. No linear relationship between the hole density and the *S* parameter is seen. An increase in the *S* parameter is typically assigned to an increase in positrons trapping to vacancy defects. However, the increased signal from positrons annihilating at vacancies could be related to either an increase in the vacancy concentration or a decrease in positrons trapping to competing negatively charged ions. In GaSb, negatively charged Ga_{Sb} are shown to effectively compete with V_{Ga} in trapping positrons at room temperature [20].

Coincidence Doppler broadening measurements were performed on a representative subset of the epitaxial layers. Positron implantation energy of 4 keV was chosen for probing the layers. Figure 3 shows the measured ratio curves. When studying materials using positron annihilation spectroscopy,

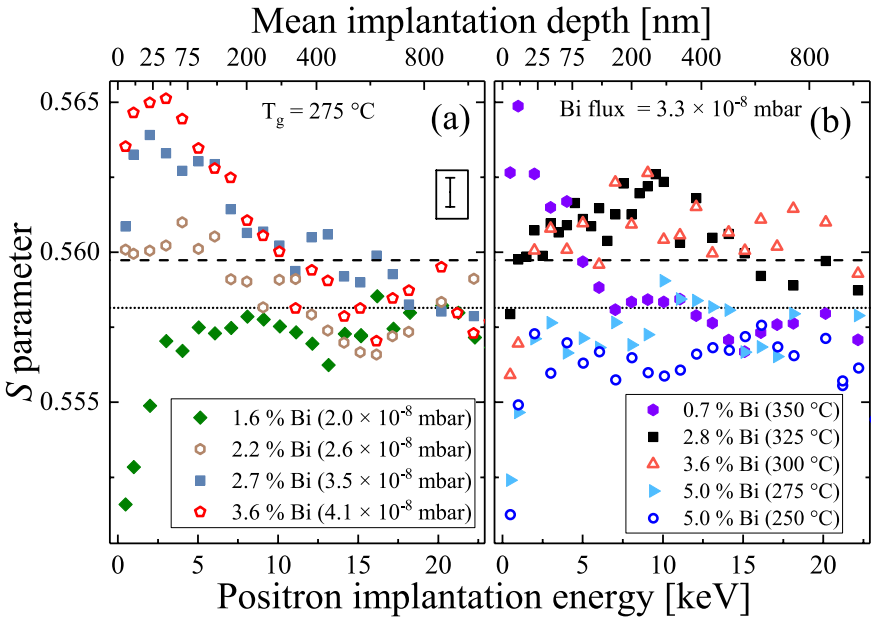

Figure 2. The *S* parameter as a function of positron implantation energy for the (a) Bi-flux and (b) growth-temperature series of $GaSb_{1-x}Bi_x$ epitaxial layers. The mean positron implantation depth is also indicated. The average value for the GaSb layers (dashed line) and *p*-type GaSb substrate value (dotted line) are also displayed. A typical error bar of the data points is shown.

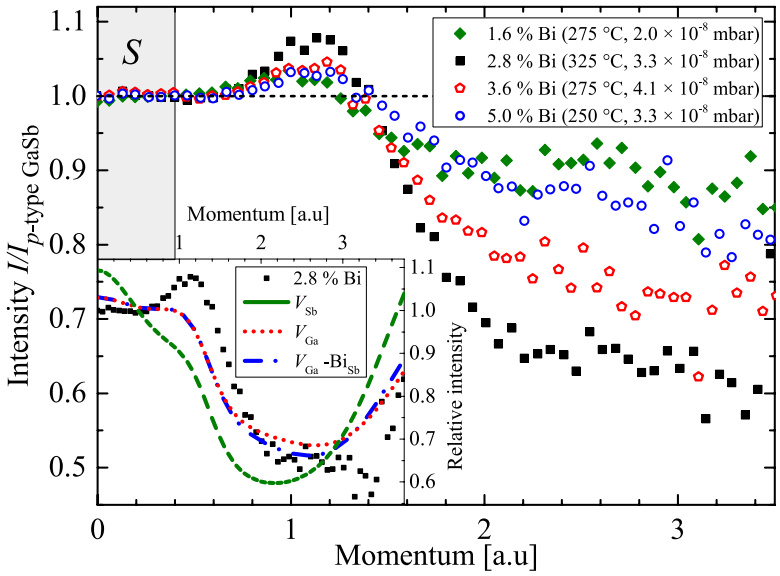

Figure 3. Measured ratio curves for two epitaxial layers from each $GaSb_{1-x}Bi_x$ series. The samples are scaled to *p*-type CZ-GaSb measured in [20] indicated as the dashed line. In the inset, calculated momentum distribution ratio curves for the V_{Sb}, V_{Ga} (calculated in [19]) and V_{Ga}-Bi_{Sb} defects compared to a measured result are shown.

the measured results are usually compared to a defect-free reference. In the case of GaSb and its ternary alloys, no suitable reference exist for this purpose since positron trapping defects are abundantly present in both undoped, *p*-type GaSb and Te-doped, *n*-type GaSb [20]. The results are therefore scaled to undoped, *p*-type, CZ-GaSb measured in [20]. The acceptor-type defect concentrations in the reference were estimated to $[Ga_{Sb}] \approx 10^{17}$ cm^{-3} and $[V_{Ga}] \approx 10^{16}$ cm^{-3}. For a more thorough discussion on the choice of the reference, see [21].

As can be seen in figure 3, the measured data of the $GaSb_{1-x}Bi_x$ layers are clearly different from those of the reference. The data show that the concentrations of positron trapping defects in these epitaxial layers are different compared to the reference. As mentioned above, the main positron trapping defect in CZ-GaSb is the Ga antisite. The ratio curve of the two epitaxial layers with the highest and lowest Bi contents have a somewhat similar intensity compared with the reference. For layers with Bi contents of 2.8% and 3.6%, the ratio curves differ distinctly from the reference displaying a clear shoulder at 1.2 a.u. and a valley at high momenta. Similar to the *S* parameter, a clear relationship between the ratio curve intensity and the hole density cannot be found.

The increase in the *S* parameter of the $GaSb_{1-x}Bi_x$ layers is an indication of an increased positron trapping into

open-volume defects. The two smallest, native, open-volume defects possibly present in the material are the Ga vacancy and the Sb vacancy (V_{Sb}). The inset of figure 3 illustrates momentum-distribution calculations of these vacancy-type structures. The two-component density-functional theory (DFT) was used for calculating the structures, employing the plane-wave code VASP [24–28]. The structures without Bi as well as the defect-free lattice used as a reference were calculated in [19]. In the same reference, the computational scheme is described in more detail.

Compared to the ratio curve of V_{Sb}, the ratio curves of the Ga-vacancy defects resemble more the measured results. The calculated signal does not change significantly if a Bi atom decorates a V_{Ga} on a neighboring Sb site (denoted V_{Ga}-Bi_{Sb}). The ratio curve of the measured data and that of the calculated Ga-vacancy defects display a low intensity at low momenta and a shoulder at momenta around 1.2 a.u. These features are clearly different for the ratio curve of the calculated V_{Sb} structure. The findings presented here are also in line with experimental results showing that the Sb vacancy is not stable in GaSb [29, 30].

Discussion

The large increase in the hole density of the studied $GaSb_{1-x}Bi_x$ layers compared to the binary material indicates an increase in the concentration of acceptor-type defects in the layers. The reason for the increased defect concentration in the layers can be related to the growth conditions. However, changes in the band structure can also have a large impact on the fraction of ionized defects. In as-grown, *p*-type GaSb, the Fermi level position in the band gap is largely defined by acceptor-type defects with ionization levels in close proximity to each other and to the valence band [20]. The band gap of the $GaSb_{1-x}Bi_x$ alloys is reported to decrease with an increasing Bi content [7–9]. A shift in the Fermi level position in relation to the acceptor-type defect ionization levels can lead to an increase in the fraction of negatively charged defects, and therefore to increased hole densities. Unidentified acceptor-type defects have previously been inferred from photoluminescence of the samples studied here [8]. However, the hole density of samples with similar Bi contents is somewhat different indicating that the growth parameters also affect the concentration of acceptor-type defects in the layers. In addition to the growth temperature and the fluxes used for the constituents, the crystallization conditions of the layers are affected by Bi atoms added to the growth [19]. This statement is supported by the results for the binary GaSb layers grown at different temperatures. The fairly similar electrical and positron result for the GaSb layers grown at different temperatures indicate that increased concentration of negatively charged defects in the $GaSb_{1-x}Bi_x$ layers does not solely depend on the growth temperature. As the Bi content in the layers is a result of the growth parameters, drawing exhaustive conclusions on the exact mechanisms behind the increased hole density is therefore challenging.

The positron data enables the identification of the acceptor-type defects present in the layers. Besides Ga vacancies, the results presented in this article imply a significant concentration of another acceptor-type defect present in the $GaSb_{1-x}Bi_x$ layers. Saturation trapping of positrons into Ga vacancies is not observed in the data. If Ga vacancies would be the sole acceptor-type defects in the layers, the measured signal should be dominated by positrons annihilating in the vacancy defects at least for the layers with hole densities in the mid-10^{18} to 10^{19} cm^{-3} range [23]. For the layer with 5% Bi, the high value on the hole density and the ratio curve of the layer similar to that of the reference indicate that another negative acceptor-type defect without open volume is present and able to compete with vacancies in trapping positrons. It can therefore be concluded that in addition to Ga vacancies acting as positron traps, negative Ga antisites are also present in the studied $GaSb_{1-x}Bi_x$ layers and contribute to the hole density.

Interestingly, a linear relationship between the positron data and the hole density is lacking. This indicates that although higher Bi content layers have higher hole densities, the proportion of the two types of acceptor-type defects contributing to the hole density is not constant. For some of the $GaSb_{1-x}Bi_x$ layers, the intensity of the ratio curve is more similar to that of the CZ-GaSb used as a reference, indicating that the Ga antisite is the dominating defect. The proportion of Ga vacancies to Ga antisites is higher in the layers for which the ratio curve differ from that of the CZ-GaSb. The concentration of the two different defects are therefore seemingly sensitive to the growth parameters and the Bi contents in the layers. However, the exact relationship between the different growth parameters, the Bi content and the concentrations of the two different acceptor-type defects cannot be concluded based on the data.

Conclusions

In conclusion, we have studied the relation between the hole density and acceptor-type defects in $GaSb_{1-x}Bi_x$ epitaxial layers. Our results show a large increase in the hole densities up to 10^{19} cm^{-3} for the $GaSb_{1-x}Bi_x$ layers compared to that of binary GaSb. Both the Ga vacancy and the Ga antisite contribute to the hole density, and the proportion of these defects vary in the $GaSb_{1-x}Bi_x$ layers. The growth parameters influence the Bi content incorporated in the alloys and the band gap, in turn, decreases with increasing Bi content. We suggest that the concentrations of acceptor-type defects in the $GaSb_{1-x}Bi_x$ layers is affected by both the reduced band gap and the growth parameters.

Acknowledgments

The calculations presented above were performed using computer resources within the Aalto University School of Science ‘Science-IT’ project. This work was partially supported by the Academy of Finland (projects 285809 and 293932). Support is acknowledged from the Engineering and Physical Sciences

Research Council, UK (Grant No. EP/G004447/2) as well as from the University of Liverpool.

References

[1] Oe K and Okamoto H 1998 *Japan. J. Appl. Phys.* **37** L1283
[2] Oe K 2002 *Japan. J. Appl. Phys.* **41** 2801
[3] Novikov S V *et al* 2012 *Phys. Status Solidi* a **209** 419–23
[4] Levander A X, Yu K M, Novikov S V, Tseng A, Foxon C T, Dubon O D, Wu J and Walukiewicz W 2010 *Appl. Phys. Lett.* **97** 141919
[5] Fluegel B, Francoeur S, Mascarenhas A, Tixier S, Young E C and Tiedje T 2006 *Phys. Rev. Lett.* **97** 067205
[6] Alberi K, Wu J, Walukiewicz W, Yu K M, Dubon O D, Watkins S P, Wang C X, Liu X, Cho Y-J and Furdyna J 2007 *Phys. Rev.* B **75** 045203
[7] Rajpalke M K, Linhart W M, Birkett M, Yu K M, Scanlon D O, Buckeridge J, Jones T S, Ashwin M J and Veal T D 2013 *Appl. Phys. Lett.* **103** 142106
[8] Kopaczek J, Kudrawiec R, Linhart W, Rajpalke M, Jones T, Ashwin M and Veal T 2014 *Appl. Phys. Express* **7** 111202
[9] Polak M P *et al* 2014 *J. Phys. D: Appl. Phys.* **47** 355107
[10] Poole I, Lee M E, Cleverley I R, Peaker A R and Singer K E 1990 *Appl. Phys. Lett.* **57** 1645–7
[11] Du M-H and Zhang S B 2005 *Phys. Rev.* B **72** 075210
[12] Ling C C, Lui M K, Ma S K, Chen X D, Fung S and Beling C D 2004 *Appl. Phys. Lett.* **85** 384–6
[13] Ma S K, Lui M K, Ling C C, Fung S, Beling C D, Li K F, Cheah K W, Gong M, Hang H S and Weng H M 2004 *J. Phys.: Condens. Matter* **16** 6205
[14] Dannefaer S, Puff W and Kerr D 1997 *Phys. Rev.* B **55** 2182
[15] Virkkala V, Havu V, Tuomisto F and Puska M J 2012 *Phys. Rev.* B **86** 144101
[16] Mahony J, Tessaro G, Mascher P, Siethoff H and Brion H G 1995 *Mater. Sci. Forum* **196–201** 1449–54
[17] Ling C C, Mui W K, Lam C H, Beling C D, Fung S, Lui M K, Cheah K W, Li K F, Zhao Y W and Gong M 2002 *Appl. Phys. Lett.* **80** 3934–6
[18] Ling C C, Fung S, Beling C D and Huimin W 2001 *Phys. Rev.* B **64** 075201
[19] Segercrantz N, Slotte J, Makkonen I, Kujala J, Tuomisto F, Song Y and Wang S 2014 *Appl. Phys. Lett.* **105** 082113
[20] Kujala J, Segercrantz N, Tuomisto F and Slotte J 2014 *J. Appl. Phys.* **116** 143508
[21] Segercrantz N, Makkonen I, Slotte J, Kujala J, Veal T D, Ashwin M J and Tuomisto F 2015 *J. Appl. Phys.* **118** 085708
[22] Rajpalke M K, Linhart W M, Yu K M, Jones T S, Ashwin M J and Veal T D 2015 *J. Cryst. Growth* **425** 241–4
[23] Tuomisto F and Makkonen I 2013 *Rev. Mod. Phys.* **85** 1583
[24] Kresse G and Furthmüller J 1996 *Phys. Rev.* B **54** 11169–86
[25] Kresse G and Furthmüller J 1996 *Comput. Mat. Sci.* **6** 15–50
[26] Kresse G and Joubert D 1999 *Phys. Rev.* B **59** 1758
[27] Makkonen I, Hakala M and Puska M J 2005 *J. Phys. Chem. Solids* **66** 1128–35
[28] Makkonen I, Hakala M and Puska M J 2006 *Phys. Rev.* B **73** 035103
[29] Segercrantz N, Slotte J, Tuomisto F, Mizohata K and Räisänen J 2017 *Phys. Rev.* B **95** 184103
[30] Bracht H, Nicols S P, Walukiewicz W, Silveira J P, Briones F and Haller E E 2000 *Nature* **408** 69–72